Front. Mater. Sci. 2023, 17(4): 230659
https://doi.org/10.1007/s11706-023-0659-3

RESEARCH ARTICLE

Preparation of PVA@PEI@BAC@CNC composite nanofibrous film with high efficiency filtration for PM2.5

Jingda Huang[1,2], Yi Wang[2], Yuxin Cai[2], Yipeng Liang[2], Shite Lin[2], Enfu Wang[2], Jinhuan Zhong[2], Wenbiao Zhang (✉)[2], and Kuichuan Sheng (✉)[1]

1 College of Biosystems Engineering and Food Science, Zhejiang University, Hangzhou 310058, China
2 College of Chemistry and Materials Engineering, Zhejiang A & F University, Hangzhou 311300, China

ABSTRACT: **It is still a challenge to prepare a water- and polymer-based electrospun air filter film with high efficiency filtration, low pressure drop, and good mechanical properties. To address this issue, polyvinyl alcohol (PVA) was employed as the main material, mixing polyethyleneimine (PEI), bamboo-based activated carbon (BAC) and cellulose nanocrystal (CNC) to construct the air filter film by electrostatic electrospinning. In this system, the negatively charged BAC and CNC are fixed in the system through bonding with the positively charged PEI, showing a double adsorption effect. One is the mechanical filtration of the porous network structure constructed by PVA@PEI electrospun nanofibers, and the other is the electrostatic adsorption of PM2.5 on the surface of BAC and CNC. It is significant that the resulting composite air filter displays a high filtration efficiency of 95.86%, a pressure drop of only 59 Pa, and good thermal stability. Moreover, the introduced methyltrimethoxysilane (MTMS) endows it with good water-resistance. Given these excellent performances, this system can provide theoretical and technical references for the development of water- and polymer-based electrospun air filter film.**

KEYWORDS: **polyvinyl alcohol; polyethyleneimine; bamboo-based activated carbon; cellulose nanocrystals; electrospun nanofibrous film; PM2.5**

Contents

Received May 19, 2023; accepted August 17, 2023

E-mails: zwb@zafu.edu.cn (W.Z.), kcsheng@zju.edu.cn (K.S.)

1 Introduction

With the development of industry, the harm of air pollution (especially PM2.5) is self-evident to human health. These regions attach great importance to the pollution and monitors its concentration regularly [1–3]. Filtering pollutants and improving air quality have always been the problems scholars have been working hard to solve until pollutants are completely controlled. Currently, there were various air filtration methods, such as effect of electric field [4–5], photocatalysis [6–7], and mechanical filtration [8–9]. However, the effect of electric field and photocatalysis methods are limited in the applications due to their high cost, cumbersome equipment, and inconvenience in carrying. Therefore, the most common method is the mechanical filtration of pollutants through porous materials [10] due to their simple preparation, easy replacement, and suitability for large-scale use. The usual porous materials for air filtration made by non-woven fabrics are mainly composed of artificially synthesized resin polypropylene. The extensive use of the synthetic resin could cause difficulties in recycling and reuse, leading to a certain burden on the environment every year [11]. Moreover, the filtration efficiency of non-woven fabrics on ultra-fine particles still needs to be improved [12]. Therefore, scholars put more effort into environmentally friendly materials for air filtration film [13–15]. In our previous research, the use of cellulose nanofibril/bamboo activated carbon composite aerogel sheet for PM2.5 filtration showed excellent filtration performance and thermostability [16]. However, the thickness of the prepared aerogel sheet was relatively large and the mechanical properties needed to be improved. Currently, it is an urgent challenge to prepare air filter using environmentally friendly materials with high filtration efficiency, low pressure drop, and good mechanical properties.

Recently, studies on electrospun nanofibers for air filtration have become a hot topic because the ultra-fine nanofibrous structures by electrostatic electrospinning [17] with a minimum diameter of 1 nm are prepared, which has a strong advantage in the adsorption of fine particles. The most typical materials for electrospun are organic solvent-based polymers. For example, ethyl acetate could be dissolved in dimethylformamide (DMF) for electrospun to prepare an air filter film with excellent filtration efficiency (over 98%) and low pressure drop (29.3 Pa) [18]. In addition, the foamed polystyrene in the mixture of DMF and d-limonene solvents was able to prepare electrospun nanofibers with stability, superhydrophobicity, high efficiency (99%), low-pressure drop (70 Pa), and quality factor of 0.16 [19]. The above shows that organic solvent-based electrospun nanofibers have good filtration performance, permeability and stability, playing an important role in the field of air filtration. However, due to the volatility of organic solvents during the electrospun process, it is inevitably of serious impact on the environment and human health. Therefore, scholars have also begun to try to use more environmentally friendly water-based polymers for electrospun. However, the water-based polymers electrospun nanofibers were usually of low strength, weak water-resistant and poor stability, and the production process was complex, limiting their application.

To overcome the drawbacks above, some scholars were dedicated to the research on compounding water-based polymer with other polymers. For example, the introduced waterproof melamine formaldehyde could improve the adjustable three-dimensional (3D) structures and the stability of polyvinyl alcohol (PVA)-based nanofibrous films by one-step electrospun and heat treatment, exhibiting excellent filtration performance (97.3% for PM0.3, 100% for PM1.0, and 100% for PM2.5) and low pressure drop (76 Pa), but the mechanical properties were not evaluated [20]. Polyacrylonitrile was added to PVA to prepare nanofibrous with small fiber diameter, pore size and good breathability by electrospun [21]. And some scholars had modified electrospun nanofibers by introducing carbon nanotubes (CNTs) as reinforcers. Wang et al. heat-bonded CNT sheets and polyimide nanofibers together by electrospun to prepare nanofibers with the highest filtration efficiency of 99% for 2.3 μm particles and low pressure drop [22]. Inorganic particles (ZnO, TiO_2, etc.) to modify electrospun nanofibers were also tried. They were introduced to PVA to prepare PVA/ZnO or TiO_2 electrospun nanofibers, which had abundant hydroxyl groups and could degrade gas pollutants into small molecules [23]. Copper acetate was crosslinked with PVA and then used to prepare PVA/Cu nanofibrous films by electrospun with high filtration efficiency of up to 99.5% for PM2.5, low pressure drop, and antibacterial properties, but the mechanical properties

were not ideal [24]. It could be known from the above that the water-based polymer electrospun nanofibrous films have good air filtration performance, and the pressure drop could be improved to some extent, but its weak mechanical strength limited its further application. Therefore, the preparation of water- and polymer-based electrospun nanofibrous films with high efficiency filtration, low pressure drop and good mechanical strength is still a serious challenge.

In our previous studies [16], bamboo-based activated carbon (BAC) has a good void structure and a certain negative charge, which could play a certain electrostatic adsorption effect on PM2.5. In addition, cellulose nanocrystals (CNC), as the biomass-reinforced material, had also made a preliminary attempt on the enhancement of the air filter film. Therefore, in this study, PVA was combined with polyethylenimine (PEI), and the introduced CNC as the reinforcer, BAC as the reinforcing adsorption and thermal stability material, and methyltrimethoxysilane (MTMS) as the hydrophobic modifier to prepare the PVA-based electrospun nanofibrous films for air filtration. The resulted PVA-based air filter was proven to be an excellent material with high filtration efficiency, good stability, low pressure drop, superior mechanical and repeatable performance, showcasing its potential to be an ideal air filter for the removal of PM2.5 in applications of environmental protection.

2 Experimental

2.1 Materials

PVA with Mw of about 85 000–98 000 (99+% hydrolyzed) was purchased from Macklin, China. PEI with the purity ⩾ 99% and molecular weight of 10 000 $g \cdot mol^{-1}$ was supplied by Aladdin, China. CNC with a solid content of 5.44% was purchased from Tianjin Muzhiling Biotechnology Co., Ltd., China. BAC (JFH400) with a diameter of 10–100 μm was provided by Zhejiang Jizhu Biotechnology Co., Ltd., China. MTMS (⩾ 98%) was purchased from Macklin, China.

2.2 Preparation of PVA@PEI@BAC@CNC composite air filter

Firstly, a certain amount of PVA powders were added into deionized water and continuously stirred in an oil bath at 100 °C for 1 h to dissolve into uniform PVA aqueous solution, and the 20% of PVA solution was obtained by adjusting the proportion of deionized water for subsequent use. And the preparation of nano BAC was briefly as follow. 30 g BAC raw material was mixed with deionized water to make 1% suspension. The speed of the supermass colloid (Masukosangyo Co., Ltd., Kawaguchi/Saitama, Japan) was set to 1500 $r \cdot in^{-1}$ and the mill spacing was 180 nm. Bamboo charcoal was ground five times to prepare nanometer bamboo charcoal and made into BAC suspension (5 wt.%).

PEI and PVA (20 wt.%) were mixed and stirred evenly, followed by adding BAC (5 wt.%) and CNC (5 wt.%) suspension, then stirred at low speed for 1 h to obtain the PVA@PEI@BAC@CNC electrospinning solution. Subsequently, under the voltage of 20.5 kV, the electrostatic spinning was carried out at the needle distance of 12 cm from the receiving plate to get the PVA@PEI@BAC@CNC composite air filter. Finally, to improve the water resistance of the PVA@PEI@BAC@CNC composite air filter, the samples stayed in a sealed bottle with MTMS were put into a 90 °C oven and modified by chemical vapor deposition (CVD) for 3 h to obtain the hydrophobic PVA@PEI@BAC@CNC composite air filter.

2.3 Characterization

The morphologies of the PVA-based air filters were observed by using field emission scanning electron microscopy (SEM; Hitachi S-4800, Japan). Fourier-transform infrared spectroscopy (FTIR; Perkin Elmer, USA) was employed to characterize the chemical structure of PVA-based air filters. The chemical state information of the samples was determined using X-ray photoelectron spectroscopy (XPS; thermo Scientific ESCALAB 250Xi). Thermal degradation analysis was examined by thermogravimetric analysis (TGA). The samples were subject to be heated at a heating rate of 10 $°C \cdot min^{-1}$ under a nitrogen atmosphere and the test temperature range was 25–1000 °C. Static water contact angle (WCA) of the samples was measured at room temperature using the water contact angle tester (JC2000D, Shanghai Zhongchen, China), then 5–8 μL droplets were placed on the sample surfaces with a micro-syringe (at least four different spots/sample, carried out in triplicate), and the average values of WCAs were evaluated.

2.4 Filtration capacity test for PM2.5

The filtration capacity of PVA-based air filters for PM2.5 was evaluated using a self-built test system described in our previous study [16]. As shown in Fig. 1, a constant air flow was driven through the smoke generating bottle via the air compressor, and the simulated PM2.5 smoke (concentration $>500\ \mu g \cdot m^{-3}$) generated by burning incense in the smoke generation bottle was passed through air filters at a velocity of $5\ cm \cdot s^{-1}$. The filtration efficiency (E) was calculated by the following equation:

$$E = \frac{N_0 - N_1}{N_0} \quad (1)$$

where N_0 and N_1 stand for the particle numbers measured without and with samples, respectively. The concentration of PM2.5 was measured by a particle counter (CEM DT-9851 M, China), and to minimize errors, all samples were measured three times and the average was taken. The pressure drop of the sample was measured by a differential pressure gauge (Testo 510, Germany) [25–26]. To evaluate the usability of the samples, the filtration efficiency and pressure drop were balanced using the following equation:

$$Q_f = -\frac{\ln(1-E)}{\Delta P} \quad (2)$$

where Q_f is an indicator of comprehensive evaluation of filtration performance, E is the filtration efficiency of PM2.5, and ΔP is the pressure drop.

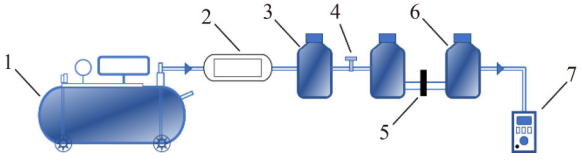

Fig. 1 Scheme of PM2.5 filtration set: air compressor (1); flowmeter (2); smoke generating bottle (3); valve (4); air filter film (5); air filtered bottle (6); particle counter (7).

2.5 Mechanical properties test

To prepare test samples, the PVA-based air filtration films were cut into the standard size of 40 mm × 10 mm (length × width). Both ends of the sample were covered with 800-grit sandpaper to create a secure grip during testing. Next, the sample was placed into the CMT6104 universal strength testing machine, ensuring a clamping distance of 20 mm with a pulling speed of $5\ mm \cdot min^{-1}$. Finally, to ensure reliable results, the average of five samples per group was taken for testing.

2.6 Regeneration of hydrophobic PVA@PEI@BAC@CNC composite air filter

Because the PVA-based air filters were easily clogged by PM2.5 after use, as previously reported in our research, MTMS was utilized as the hydrophobic modifier to enable its water resistance. To test the efficacy of this modification, the used samples were immersed in water and swung gently for 30 s to be effectively cleaned.

2.7 Heat resistance test

To evaluate the heat resistance, PVA-based composite air filters were dried at room temperature, 50, 100, and 150 °C for 2 h, respectively, and the filtration efficiency, pressure drop, and WCA of each sample were measured.

3 Results and discussion

3.1 Forming and working mechanism of PVA@PEI@BAC@CNC composite air filter

Figure 2(a) shows the forming and working mechanism of the PVA@PEI@BAC@CNC composite air filter prepared by electrostatic spinning. Due to its excellent biocompatibility, PEI was introduced to the PVA solution, and its merits of high adhesion, high adsorption, and high reactivity could give nanofibrous better versatility. CNC and BAC carried negative charges and could be electrostatic bonded with positively charged PEI fibers during spinning. After treating with MTMS by CVD, the air filter displayed good hydrophobicity.

In the PVA@PEI@BAC@CNC system, a dual filter structure was constructed. First, the interception of PM2.5 by the electrospun nanofibrous network structure constructed by PVA@PEI. Second, there was the electrostatic adsorption between the surface negative charge of both BAC and CNC and the surface positive charge of PM2.5, resulting in the high filtration efficiency of the PVA-based air filtration. The added BAC was benefit to prevent nanofibrous bonding with each other to some extent, which might be due to the fact that the particle size of BAC was larger than the nanofibrous diameter and could play a role in expanding and supporting electrospun nanofibers, as well as increasing the porosity, so the pressure drop could be effectively

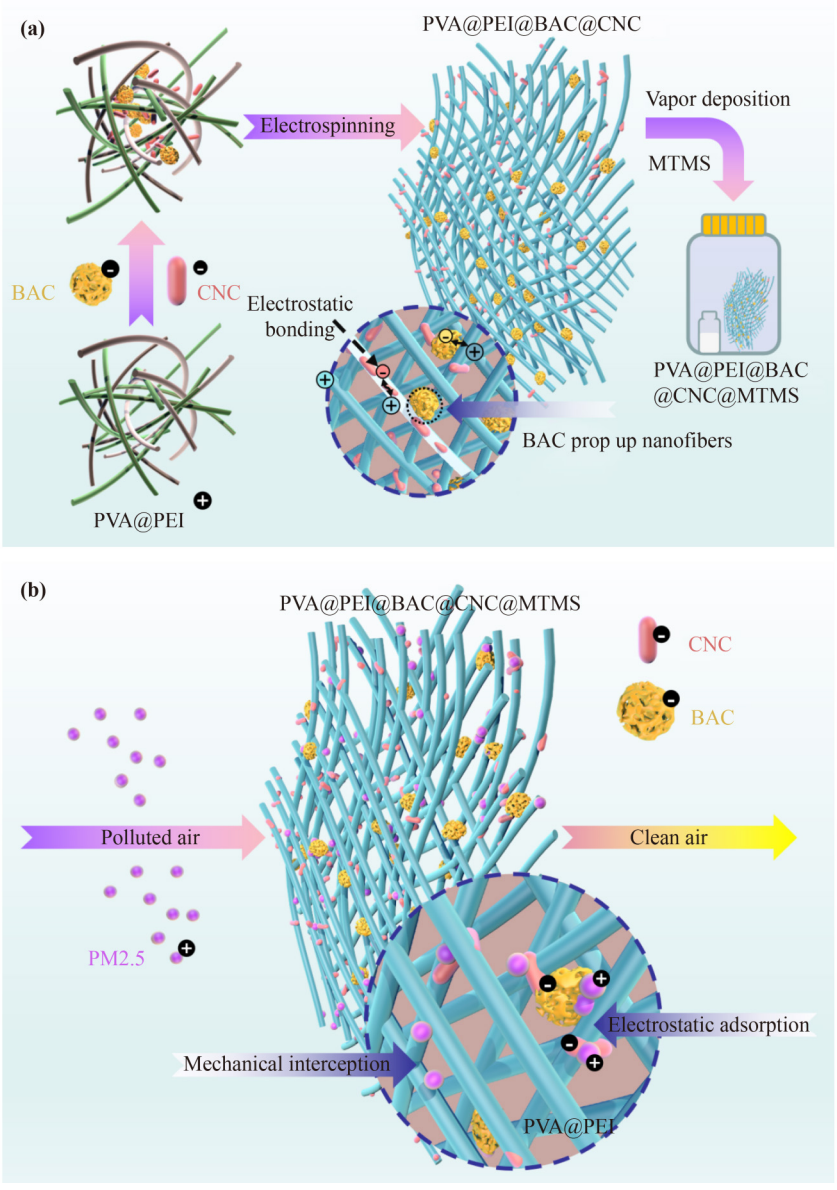

Fig. 2 (**a**) Forming mechanism and (**b**) PM2.5 filtration principle of the PVA@PEI@BAC@CNC composite air filter.

reduced. CNC, as an environmentally friendly nano-reinforced material, can improve the mechanical properties of the system due to its high crystallinity. After the MTMS modification, it gave the system hydrophobicity and enhanced its water resistance. Based on above processes, the PVA@PEI@BAC@CNC@MTMS composite air filter was endowed with good mechanical properties, high filtration efficiency, and low pressure drop.

3.2 Morphological analysis

As shown in Fig. 3(a), the inner structure of pure PVA electrospun nanofibers exhibits an irregular 3D network structure and could effectively intercept solids of a certain size, which is very suitable for the removal of PM2.5. The introduction of PEI makes the network structure more compact (Fig. 3(b)) because the viscosity of PEI enhances the binding force among electrospun nanofibers. Figure 3(c) shows that BAC is successfully introduced and encapsulated by PVA@PEI, which enhances the stability of BAC in the system. On the other hand, proper amount of BAC could prevent the agglomeration of electrospun nanofibers and play a certain role in reducing the pressure drop. As shown in Fig. 3(d), part of CNC is agglomerated and uniformly distributed on the

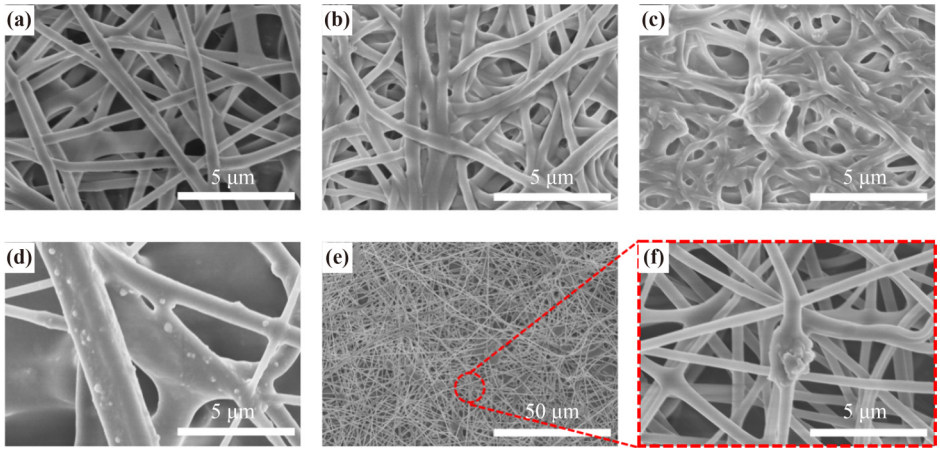

Fig. 3 SEM images of (**a**) PVA, (**b**) PVA@PEI, (**c**) PVA@PEI@BAC, and (**d**) PVA@PEI@BAC@CNC composite air filtration. (**e**) SEM image and (**f**) its high magnification of the hydrophobic PVA@PEI@BAC@CNC composite air filtration.

nanofibrous surface, significantly improving the network structures of the system. And the surface negative charge of CNC could effectively produce electrostatic adsorption on PM2.5. After the modification with MTMS, as shown in Figs. 3(e) and 3(f), the hydrophobic PVA@PEI@BAC@CNC composite electrospun nanofibers form a regular and uniform network structure due to the cover of MTMS to CNC agglomeration. In this system, BAC is well loaded on nanofibers, MTMS completely encapsulates PEI, PVA, BAC, and CNC, which is of good porosity and more conducive to the PM2.5 adsorption and the reduction of pressure drop after filtration.

3.3 Chemical component analysis

During the preparation process of PVA-based electrospun nanofibers, the change of both chemical composition and structure was analyzed by FTIR. As shown in Fig. 4, the characteristic peaks of pure PVA electrospun nanofibers appear at 3300 cm^{-1} (−OH stretching vibration), 2930 cm^{-1} (C−H stretching vibration) [27], and 1090 cm^{-1} (C−O asymmetric stretching vibration), respectively. After adding PEI, there are new characteristic peaks observed on the PVA@PEI one at 1560 cm^{-1} (C−N stretching vibration), 1630 cm^{-1} (N−H bending vibration) [28], 1310 cm^{-1} (C−N stretching and bending vibration) and 815 cm^{-1} (N−H out-of-plane deformation vibration) [29–30], which are all the characteristic peaks of PEI, proving only physical mixing between PVA and PEI. The peak at 3300 cm^{-1} is stronger than that of pure PVA film due to the superposition of the N−H peak of PEI. Because the characteristic peaks of CNC, BAC, and PVA basically overlap with each other,

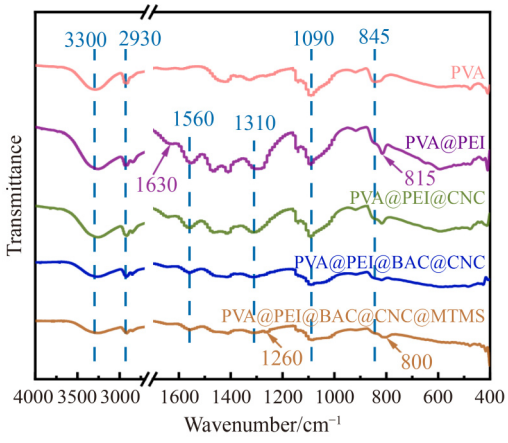

Fig. 4 FTIR spectra of different PVA-based electrospun nanofibrous films.

no new characteristic peaks appear in the PVA@PEI@BAC@CNC electrospun nanofibrous. In contrast, after modification with MTMS, new characteristic peaks appear at 1260 cm^{-1} (C−H of MTMS) and 800 cm^{-1} (Si−C and Si−O−Si), indicating the successful modification of MTMS [31].

XPS was further employed to analyze the chemical composition of different PVA-based electrospun nanofibrous films. As shown in Fig. 5(a), the presence of element N (400 eV) confirms the successful introduction of PEI. The elements C and O derive from PVA, PEI, CNC, and BAC, while the element Si is mainly from MTMS. Based on the C 1s spectra in Figs. 5(b)–5(e), it could be observed that only C−C, C−H, and C−OH bonds are exhibited by PVA, while C−N bond appears after the introduction of PEI, confirming the successful composite of PEI and the consistence with the element contents

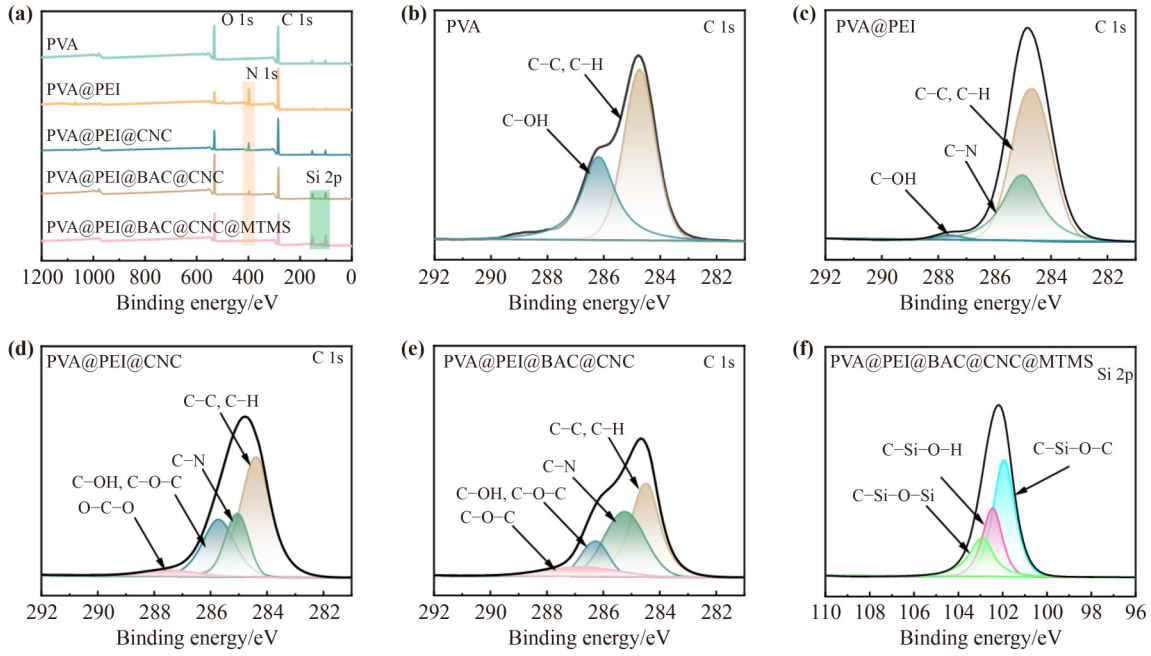

Fig. 5 (**a**) XPS spectra of PVA-based electrospun nanofibrous films. C 1s spectra of (**b**) pure PVA, (**c**) PVA@PEI, (**d**) PVA@PEI@CNC, and (**e**) PVA@PEI@BAC@CNC electrospun nanofibrous films. (**f**) Si 2p spectrum of hydrophobic PVA@PEI@BAC@CNC electrospun nanofibrous films.

revealed in Table 1. Figure 5(d) shows the presence of C−O−C and O−C−O bonds, which came from CNC, indicating the successful incorporation of CNC. The chemical bonds of BAC were similar to those of PVA@PEI@BAC@CNC electrospun nanofibrous films (Fig. 5(e)). But as shown in Table 1, a trace amount of silicon is found after introducing BAC, which might originate from the ash content in BAC. Figure 5(f) shows the C 1s spectrum of the hydrophobic PVA@PEI@BAC@CNC composite electrospun nanofibrous films, exhibiting C−Si−O−C, C−Si−O−H, and C−Si−O−Si bonds and indicating the successful modification with PDMS, which would also be confirmed by in the following WCA test (as shown in Figs. 8(e) and 8(f)).

Table 1 Element content ratios of different PVA-based electrospun nanofibrous films

Sample	Atomic content/%				*c*(C)/*c*(O)
	C	O	N	Si	
PVA	77.65	22.35	–	–	3.47
PVA@PEI	71.83	10.16	18.01	–	7.07
PVA@PEI@CNC	73.82	16.89	9.30	–	4.37
PVA@PEI@BAC@CNC	57.43	29.29	3.73	9.55	1.96
PVA@PEI@BAC@CNC@MTMS	58.21	22.31	1.77	17.71	2.61

3.4 Thermal stability analysis

Thermal stability is one of the main indexes of materials. As shown in Fig. 6(a), as PVA is the main material, all the samples show a TGA curve with the similar tendency, and before 100 °C, the mass loss is mainly due to the evaporation of water. In the pure PVA electrospun nanofibrous, during 100–240 °C, the weight loss occurs because of the evaporation of crystalline water in the molecular chain. It is followed by the thermal decomposition between 250 and 380 °C with the fastest rate observed at 294 °C (Fig. 6(b)), which is due to the rapid weight loss caused by the scission of PVA chain segments. The final residual mass is only 0.3%, indicating the poor heat resistance of pure PVA. Similarly, the other samples with the addition of PEI undergo decomposition between 100 and 220 °C for the same reasons as pure PVA. Subsequently, the decomposition continues between 200 and 280 °C, caused by the degradation of PEI molecular chain side chains. The third decomposition phase occurred between 300 and 450 °C, with the main chain of PEI breaking down and reaching the highest degradation rate at 386 °C. The heat resistance of the samples is improved after the added PEI. It is noteworthy that the introduced CNC results in a decrease in residual mass due to the poor heat resistance of CNC as a kind of biomass material, while the added BAC increase the

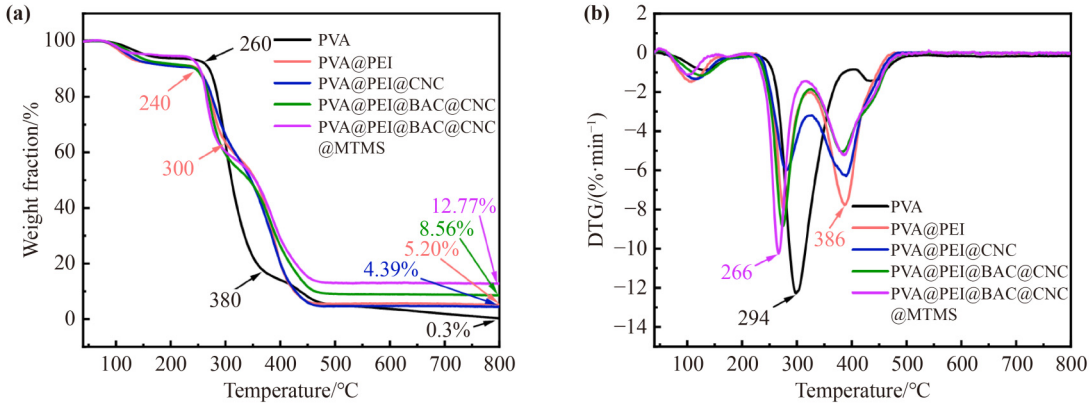

Fig. 6 (**a**) TGA and (**b**) DTG curves of different PVA-based electrospun nanofibrous films.

residual mass. This is attributed to the lower thermal decomposition rate of BAC, indicating that BAC is helpful in improving heat resistance of the system. The subsequent introduction of MTMS leads to a reduction of weight loss at every stage of the sample due to the protective role of the C layer formed after its pyrolysis, with a significantly higher final residual mass compared to other samples (reaching 12.77%). From above, the introduced BAC could enhance the thermal stability of the system.

3.5 Mechanical properties analysis

The mechanical properties are closely related to the application field and range of electrospun nanofibrous films. In particular, the mechanical strength of the usual water- and polymer-based electrospun nanofibrous film is relatively poor, so it is very important to improve its strength. In this system, to demonstrate the effects of the components on the PVA-based electrospun nanofibrous films, the tensile tests were carried out. As shown in Fig. 7(a), the stress of pure PVA electrospun nanofibrous film is 3.2 MPa, but the fracture strain is only 29%. The introduced PEI makes the electrospun nanofibrous films more compact in structure by lots of hydrogen bonding and greatly enhances the fracture strain of the nanofibrous films, but the stress decreases somewhat. The added CNC greatly improves the toughness of the composite nanofibrous films and the fracture strain is up to 93%, resulting from the high strength of CNC and its high specific surface area, which could produce hydrogen bonding with PVA and PEI. But the stress further decreases to only 1.9 MPa, which might be caused by the introduced CNC blocked the integration of PVA and PEI to a certain extent. The introduced BAC significantly reduces the toughness of the nanofibers and makes an increase in stress, which is benefited from the rigidity of BAC, but showing a fracture strain of 30%, which might result from the barrier effect of BAC particles on polymer chains. After the modification with MTMS, MTMS completely covers the surface of the composite nanofibrous films and the stress reaches 4.3 MPa,

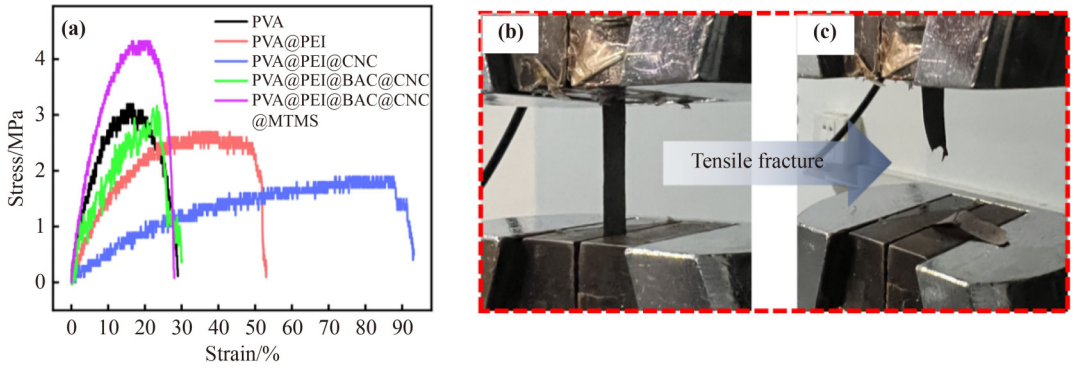

Fig. 7 (**a**) Tensile stress–strain curves of PVA-based electrospun nanofibrous films. Pictures of (**b**) pre-fracture and (**c**) post-fracture of hydrophobic PVA@PEI@BAC@CNC electrospun nanofibrous film.

indicating that the hydrophobic PVA@PEI@BAC@CNA composite electrospun nanofibrous film has excellent mechanical strength.

3.6 Filtration performance analysis

Large amounts of PM2.5 are produced in industrial production, and as a result, PM2.5 filter have received widespread attention in recent years. To test the filtration efficiency of the PVA-based electrospun nanofibrous films in an imitation of the polluted environment, a self-built filtration system was designed for testing. As shown in Fig. 8(a), the pure PVA electrospun nanofibrous film

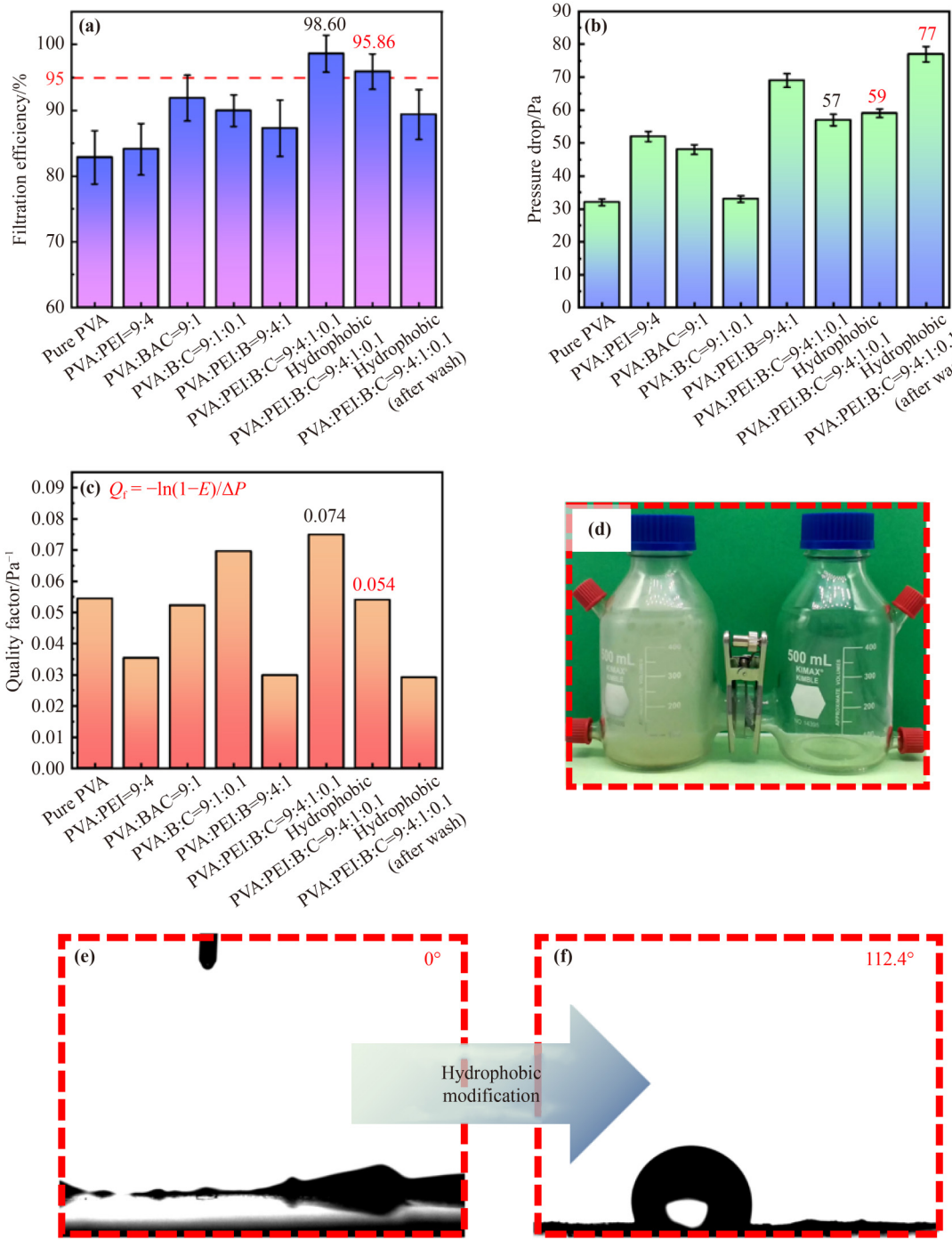

Fig. 8 (**a**) Filtration efficiency, (**b**) pressure drop, and (**c**) Q_f of different PVA-based electrospun nanofibrous films for PM2.5 under the gas velocity of 5 cm·s^{-1}. (**d**) Picture for barrier of sample to PM2.5. WCAs of PVA@PEI@BAC@CNC (**e**) before and (**f**) after the modification.

shows a filtration efficiency of only 82.84%, which might be because the pore sizes of the film were large and part of PM2.5 could penetrate it. It could be known from SEM analysis above, the addition of PEI leads to the enhancement of the adhesion among electrospun nanofibers due to its high viscosity, and a little increase in the filtration efficiency of PVA@PEI one due to the reduced pore sizes. The PVA@PEI@BAC one shows an increase in filtration efficiency compared with the one without BAC since BAC itself is of high porosity, as well as reducing the adhesion caused by PEI and increasing the porosity in the system. Additionally, BAC is negatively charged and able to adsorb PM2.5 through electrostatic adsorption. After the addition of CNC, the filtration efficiency reached the maximum of 98.60% due to rich negative charges in the CNC surface for the removal of PM2.5 with electrostatic adsorption. Compared with other electrospun films, it also has certain advantages, as shown in Table 2 [32–33].

In order to enhance the water resistance of the PVA-based electrospun nanofibrous films in humid environment, MTMS was employed to prepare the hydrophobic PVA@PEI@BAC@CNC composite electrospun nanofibrous film, showcasing the increase of WCA to 112.4° (Fig. 8(f)). However, the filtration efficiency slightly decreases due to MTMS blocking some small pores and its hydrophobicity decreasing the interception of PM2.5. The quality factor (Q_f) of the hydrophobic PVA@PEI@BAC@CNC composite electrospun nanofibrous film is 0.074 (Fig. 8(c)), with a filtration efficiency of 95.86% and a WCA of 112.4°, indicating that the hydrophobic PVA@PEI@BAC@CNC one had good filtration performance and water resistance.

Figure 9(a) shows the SEM image of the hydrophobic PVA@PEI@BAC@CNC composite electrospun nanofibrous films before filtering PM2.5. However, after five cycles of the filtration of PM2.5, the nanofibrous arrangement becomes disordered and irregular, which hinders the filtration efficiency of PM2.5 (Fig. 9(b)). After water washing (Fig. 9(c)), the filtration efficiency retains 89% (Fig. 8(a)). Because the original regular structure of the composite electrospun nanofibrous film is destroyed in the process of water washing, the PVA nanofibers squeeze each other, which increases the pressure drop (77 Pa) and reduces Q_f to 0.029 (Fig. 8(c)).

To verify the heat resistance of the hydrophobic PVA@PEI@BAC@CNC composite electrospun nanofibrous film, the samples were held in an oven for 2 h at room temperature and 50, 100, and 150 °C, respectively, to test filtration efficiency, pressure drop and WCAs. As shown in Fig. 10(a), with the increased temperature, the overall filtration efficiency presents a certain downward trend, from 95.86% to 82.88%. However, the pressure drop gradually increases, and the pressure drop reaches 104 Pa when the temperature reaches 150 °C. This is because with the increase of temperature, PVA might melt to a certain extent, causing local structure collapse and even plugging pores, thus leading to the reduction of the filtration efficiency and the increase of the pressure drop. The wettability of the hydrophobic material PVA@PEI@BAC@CNC is less affected by the increase of temperature, and the WCA ranges from 112.3° to 125.1°. Therefore, under the heating condition of 100 °C, the filtration efficiency of the hydrophobic PVA@PEI@BAC@CNC one remains above 90% and shows excellent heat resistance.

Table 2 Comparison with other electrospun films

Sample	Filtration efficiency/%	Pressure drop/Pa	Mechanical property/MPa	Ref.
PEPNF5-90	> 94	18	–	[32]
zein@ZIF-8	> 95	54.87	0.014	[33]
This work	95.86	59	4.3	–

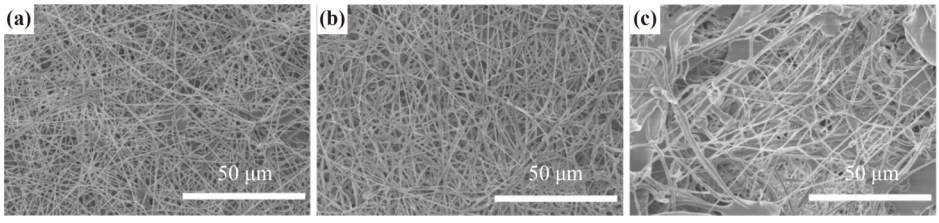

Fig. 9 SEM images of hydrophobic PVA@PEI@BAC@CNC composite electrospun nanofibrous films: (**a**) before filtration, (**b**) after filtration, and (**c**) after water washing for 5 times.

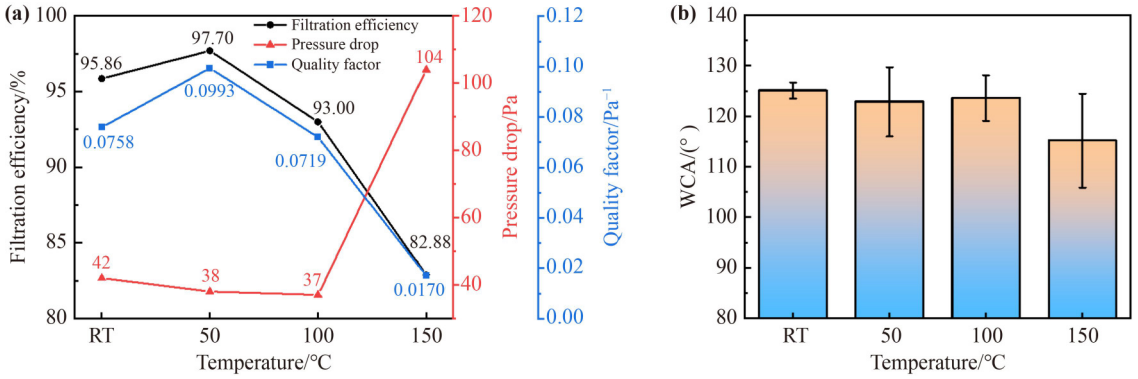

Fig. 10 Values of (**a**) filtration efficiency/pressure drop/quality factor and (**b**) WCAs of hydrophobic PVA@PEI@BAC@CNC composite electrospun nanofibrous films at room temperature and 50, 100, and 150 °C.

4 Conclusion

In summary, it is feasible to synthesize PEI, BAC, and CNC with PVA for the preparation of environmentally friendly composite electrospun nanofibrous films for the removal of PM2.5. In this system, PVA and PEI spinning construct multiple particle junction to play a major role in filtering PM2.5. PEI could enhance the viscosity of the system and had positive charge, which is conducive to strong adhesion of the negatively charged CNC and BAC in the system. BAC is conducive to enhancing the porosity of the system, CNC is benefit for the improvement of the toughness of the system, and the negative charge on the surface is conducive to enhancing the filtration efficiency of the system through electrostatic adsorption. The hydrophobic modification endowed the system with water resistance, the filtration efficiency of the composite electrospun nanofibrous film was as high as 95.86%, the pressure drop of only 59 Pa, and the Q_f of 0.074. This study could supply a simple and effective strategy with environmental protection for high efficiency filtration for PM2.5.

Declaration of competing interests The authors declare that they have no competing interests.

Acknowledgements Project funded by the China Postdoctoral Science Foundation (No. 2021M692806), the Natural Science Foundation of Zhejiang Province (No. LY21C160002), and the Scientific Research Development Foundation of Zhejiang A & F University (No. 2018FR054).

References

[1] Lelieveld J, Evans J S, Fnais M, et al. The contribution of outdoor air pollution sources to premature mortality on a global scale. Nature, 2015, 525(7569): 367–371

[2] Pui D Y H, Chen S C, Zuo Z. PM2.5 in China: measurements, sources, visibility and health effects, and mitigation. Particuology, 2014, 13: 1–26

[3] Anwar M N, Shabbir M, Tahir E, et al. Emerging challenges of air pollution and particulate matter in China, India, and Pakistan and mitigating solutions. Journal of Hazardous Materials, 2021, 416: 125851

[4] Yang D, Liu Z, Yang P, et al. A curtain purification system based on a rabbit fur-based rotating triboelectric nanogenerator for efficient photocatalytic degradation of volatile organic compounds. Nanoscale, 2023, 15(14): 6709–6721

[5] Zhu C, Yang F, Xue T, et al. Metal-organic framework decorated polyimide nanofiber aerogels for efficient high-temperature particulate matter removal. Separation and Purification Technology, 2022, 300: 121881

[6] Sohara K, Yamauchi K, Sun X, et al. Photocatalytic degradation of polycyclic aromatic hydrocarbons in fine particulate matter (PM2.5) collected on TiO_2-supporting quartz fibre filters. Catalysts, 2021, 11(3): 400

[7] Shiraki K, Yamada H, Yoshida Y, et al. Improved photocatalytic air cleaner with decomposition of aldehyde and aerosol-associated influenza virus infectivity in indoor air. Aerosol and Air Quality Research, 2017, 17(11): 2901–2912

[8] Sukchai P, Wanwong S, Wootthikanokkhan J. Electrospun cellulose air filter coated with zeolitic imidazolate frameworks (ZIFs) for efficient particulate matter removal: effect of coated ZIFs on filtration performance. Fibers and Polymers, 2022, 23(5): 1206–1216

[9] Kim H J, Kim Y J, Seo Y J, et al. Hybrid bead air filters with low pressure drops at a high flow rate for the removal of particulate matter and HCHO. Polymers, 2022, 14(3): 422

[10] Zhang H, Liu J, Zhang X, et al. Design of electret polypropylene

melt blown air filtration material containing nucleating agent for effective PM2.5 capture. RSC Advances, 2018, 8(15): 7932–7941

[11] Liu C, Dai Z, He B, et al. The effect of temperature and humidity on the filtration performance of electret melt-blown nonwovens. Materials, 2020, 13(21): 4774

[12] Li J, Gao F, Liu L Q, et al. Needleless electro-spun nanofibers used for filtration of small particles. Express Polymer Letters, 2013, 7(8): 683–689

[13] Ryu J, Kim J J, Byeon H, et al. Removal of fine particulate matter (PM2.5) via atmospheric humidity caused by evapotranspiration. Environmental Pollution, 2019, 245: 253–259

[14] Chen J, Zhou Z, Miao Y, et al. Preparation of CS@BAC composite aerogel with excellent flame-retardant performance, good filtration for PM2.5 and strong adsorption for formaldehyde. Process Safety and Environmental Protection, 2023, 173: 354–365

[15] Li C L, Song W Z, Sun D J, et al. A self-priming air filtration system based on triboelectric nanogenerator for active air purification. Chemical Engineering Journal, 2023, 452: 139428

[16] Zhao K, Ren C, Lu Y, et al. Cellulose nanofibril/PVA/bamboo activated charcoal aerogel sheet with excellent capture for PM2.5 and thermal stability. Carbohydrate Polymers, 2022, 291: 119625

[17] Biranje S, Madiwale P, Adivarekar R V. Electrospinning of chitosan/PVA nanofibrous membrane at ultralow solvent concentration. Journal of Polymer Research, 2017, 24(6): 92

[18] Han W, Rao D, Gao H, et al. Green-solvent-processable biodegradable poly(lactic acid) nanofibrous membranes with bead-on-string structure for effective air filtration: “Kill two birds with one stone”. Nano Energy, 2022, 97: 107237

[19] Rajak A, Hapidin D A, Iskandar F, et al. Controlled morphology of electrospun nanofibers from waste expanded polystyrene for aerosol filtration. Nanotechnology, 2019, 30(42): 425602

[20] Yan G, Yang Z, Li J, et al. Multi-unit needleless electrospinning for one-step construction of 3D waterproof MF-PVA nanofibrous membranes as high-performance air filters. Small, 2023, 19(7): 2206403

[21] Yardimci A I, Kayhan M, Tarhan O. Polyacrylonitrile (PAN)/polyvinyl alcohol (PVA) electrospun nanofibrous membranes synthesis, characterizations, and their air permeability properties. Journal of Macromolecular Science Part B: Physics, 2022, 61(10–11): 1426–1435

[22] Wang Q, Yildiz O, Li A, et al. High temperature carbon nanotube — nanofiber hybrid filters. Separation and Purification Technology, 2020, 236: 116255

[23] Khan M Q, Kharaghani D, Ullah S, et al. Self-cleaning properties of electrospun PVA/TiO_2 and PVA/ZnO nanofibers composites. Nanomaterials, 2018, 8(9): 644

[24] des Ligneris E, Dumée L F, Al-Attabi R, et al. Mixed matrix poly (vinyl alcohol)–copper nanofibrous anti-microbial air-microfilters. Membranes, 2019, 9(7): 87

[25] Nemoto J, Saito T, Isogai A. Simple freeze-drying procedure for producing nanocellulose aerogel-containing, high-performance air filters. ACS Applied Materials & Interfaces, 2015, 7(35): 19809–19815

[26] Zhang S, Tanioka A, Okamoto M, et al. High-quality nanofibrous nonwoven air filters: additive effect of water-jet nanofibrillated celluloses on their performance. ACS Applied Polymer Materials, 2020, 2(7): 2830–2838

[27] Abid Z, Hakiki A, Boukoussa B, et al. Preparation of highly hydrophilic PVA/SBA-15 composite materials and their adsorption behavior toward cationic dye: effect of PVA content. Journal of Materials Science, 2019, 54(10): 7679–7691

[28] Chen Y, Cao J, Wei H, et al. Fabrication of AgNPs decorated on electrospun PVA/PEI nanofibers as SERS substrate for detection of enrofloxacin. Journal of Food Measurement and Characterization, 2022, 16(3): 2314–2322

[29] Majumdar S S, Das S K, Saha T, et al. Adsorption behavior of copper ions on *Mucor rouxii* biomass through microscopic and FTIR analysis. Colloids and Surfaces B: Biointerfaces, 2008, 63(1): 138–145

[30] Choi J H, Hong Y P, Park Y C. Spectroscopic and ligand-field properties of [L-prolylglycinato][di(3-aminopropyl) amine] chromium(III) perchlorate. Spectrochimica Acta Part A: Molecular and Biomolecular Spectroscopy, 2002, 58(8): 1599–1606

[31] Liu Y, Huang Y, Huang Q, et al. Liquid-phase deposition functionalized wood sponges for oil/water separation. Journal of Materials Science, 2021, 56(34): 19075–19092

[32] Kim H J, Park S J, Park C S, et al. Surface-modified polymer nanofiber membrane for high-efficiency microdust capturing. Chemical Engineering Journal, 2018, 339: 204–213

[33] Zhang J, Lu Q, Ni R, et al. Spiral grass inspired eco-friendly zein fibrous membrane for multi-efficient air purification. International Journal of Biological Macromolecules, 2023, 245: 125512